Available online at www.sciencedirect.com
SCIENCE DIRECT
Journal of Power Sources 158 (2006) 143–147
JOURNAL OF POWER SOURCES
www.elsevier.com/locate/jpowsour

Design of low-humidification PEMFC by using cell simulator and its power generation verification test☆

Y. Yoshikawa, T. Matsuura, M. Kato, M. Hori *

Fuel Cell Laboratory, Daido Institute of Technology, 10-3 Takiharu-cho, Minami-ku, Nagoya 457-8530, Japan

Received 31 May 2005; received in revised form 4 October 2005; accepted 4 October 2005
Available online 28 February 2006

Abstract

As long as the perfluorinated proton exchange membrane (PEM) is used for the electrolyte, both the cell performance and life are highly dependent upon the water content in the electrolyte. On the other hand, pre-humidification of fuel and oxidant gases complicates the PEMFC system and prevents it from possible cost reduction measures. In this study, in order to maintain a membrane electrode assembly (MEA) with a satisfactory water content by only the water produced in catalyst layer through the electrode reaction without prior humidification of both the fuel and oxidant gases, a novel gas diffusion layer (GDL) was fabricated. This was achieved by coating a water management layer (WML) onto a traditional GDL in order to place the WML between the traditional GDL and the catalyst layer of the PEMFC. This study describes the significant balance of water with WML in the fuel cell using both simulation and experimental analysis.

Keywords: Proton exchange membrane fuel cell; Water management; Porous media; Simulation analysis

1. Introduction

Perfluorosulfonate ion-exchange resin is typically used for the electrolyte membrane of a proton exchange membrane fuel cell (PEMFC) [1–2]. In order to obtain a high cell voltage using this membrane, a high humidity must be maintained [3–7]. However, too high humidity causes flooding of electrode. Both flooding and dehydration are well-known factors that negatively affect the performance of PEMFC [8–10]. And both simplification and cost reduction to the PEMFC system as well as improvements to reduce the cell start-up time can be achieved by humidifying the electrolyte membrane with the water produced in the cathode catalyst layers through an electrode reaction and by operating at as low a humidity of fuel and oxidant feedstreams as possible [17]. To fulfill this goal, a water management layer (WML) was installed between the catalyst layer (CL) and gas diffusion layer (GDL) of the PEMFC [11–16]. Optimization of the low humidity of the fuel and oxidant feedstreams is thereby achieved by controlling the movement of generated water to the outside of the cell.

In this study, as part of the above-mentioned investigation, the vapor permeation rate through the WML-coated GDL necessary to achieve low cell humidification was experimentally calculated with the reported cell simulator [18] and the vapor permeation rate through various porous media was evaluated. Then, power generation tests were conducted on a single cell in which a WML of selected material had been incorporated. As a result, the lowest possible humidification cell was attained.

2. Cell simulator

A flow chart of the cell simulator is shown in Fig. 1 [18]. The simulator allows for the phenomena inside the cell to be mathematically analyzed by coupling the electrode reactions, mass transfer and heat transfer including both evaporation and condensation.

Distributions of current density, temperature and gas composition are two-dimensionally calculated in a cell plane. And

Presented at the Fuel Cell Seminar 2–4 November 2004. The reference title of the abstract is Development of Self-humidified Membrane Electrode Assembly with a Novel Gas Diffusion Layer for PEMFC.

* Corresponding author. Tel.: +81 52 612 6111x2508; fax: +81 52 612 5623.
E-mail address: hori@daido-it.ac.jp (M. Hori).

0378-7753/$ – see front matter © 2005 Elsevier B.V. All rights reserved.
doi:10.1016/j.jpowsour.2005.10.003

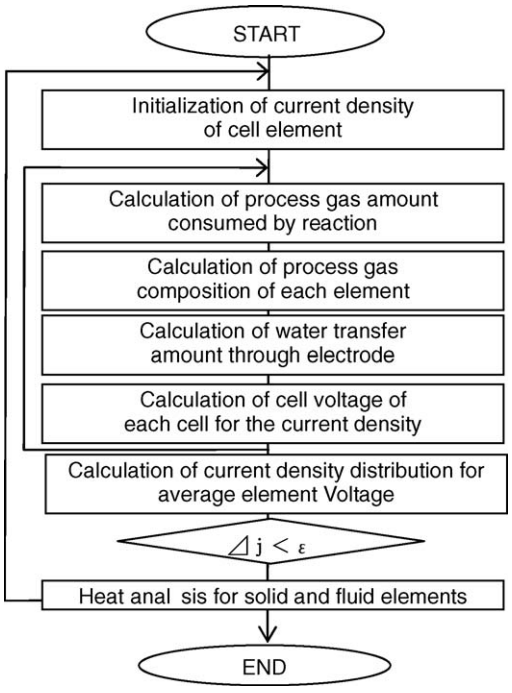

Fig. 1. Flow chart of cell simulator.

mass transfer of hydrogen, oxygen, proton, water and vapor in MEA are one-dimensionally calculated in a stacking direction of cell parts such as a membrane, catalyst layer and gas diffusion layers. By combining the two-dimensional calculation in a cell plane with the one-dimensional calculation in a cell stacking direction, phenomena in cell three-dimensionally simulated.

In this cell simulator, the WML is coated onto a traditional GDL so that it can be inserted between the anode and cathode's catalyst layer and GDL, and the movement of the generated water to the outside of the cell is controlled. Thus, the goal was to maintain the polymer membrane and the catalyst layer in a humid state. In this analysis model, the vapor permeation rate, dn/dt (mol s^{-1} m^{-2}), through the GDL or the WML-coated GDL can be expressed in the following equation [20]:

$$\frac{dn}{dt} = \frac{1}{1-\omega} n D \frac{\partial \omega}{\partial y} \quad (1)$$

Here ω is the mole fraction of water vapor in humidified air, D the diffusion coefficient of water vapor through GDL or WML-coated GDL (m^2 s^{-1}), n the mole density of water vapor (mol m^{-3}), y the stacking direction of cell parts, and t is the time (s).

3. Design of low humidification cell with simulator

The cell simulator described in Section 2 was used to evaluate the optimum vapor permeation rates through the GDL or WML-coated GDL for a cell with a reaction area of 3 cm × 15 cm. The purpose of this configuration is to maintain the catalyst layers, which are located on both sides of the polymer membrane, at a high humidity using only the reaction-generated water.

Table 1
Analytical conditions for cell stack

Active area	0.03 m × 0.15 m
Operating pressure	Ambient
Cell temperature (°C)	80
Flow field	
Fuel	Straight
Oxidant	Straight
Gas flow direction	Co-flow
Gas composition	
Fuel	$H_2 + CO_2$ (20%)
Oxidant	Air
Current density	0.4 A cm^{-2}
Utilization (%)	
Fuel	70
Oxidant	40
Humidification temperature (°C)	
Fuel	60
Oxidant	40

3.1. Analytical conditions

The analytical conditions for the cell stack are shown in Table 1. For this analysis, a stack with an active area of 3 cm × 15 cm was assumed, and only a single cell with insulated boundary conditions on both sides was used as the model, in order to represent one of the stacked multi-cells. As shown in the table, the operation pressure was atmospheric pressure and the cell temperature was 80 °C. The gas composition of the fuel was that obtained by methane reforming, and is shown in the following equation:

$$CH_4 + 3H_2O \rightarrow 4H_2 + CO_2 + H_2O \quad (2)$$

The utilization of fuel was 70%. The oxidant was air that is humidified at a relatively low temperature, 40 °C, with a utilization of 40%. The current density was fixed at 0.4 A cm^{-2}. The water diffusion coefficient through the membrane was fixed as $D/\partial y = 2.0 \times 10^{-2}$ m s^{-1} divided by a membrane thickness, which was experimentally obtained in a water permeation test of the same kind of membrane as used in power generation test [17].

3.2. Analysis results

Fig. 2(a) and (b) shows the relationship between the relative humidity and $D/\partial y$ of Eq. (1). The relative humidity is plotted for fuel, oxidant, the anode catalyst layer, and the cathode catalyst layer at both the oxidant inlet and outlet, which were all obtained from the simulation analysis. As shown in the figure, a vapor permeation rate of the GDL or WML-coated GDL at the oxidant inlet and outlet should be set to $D/\partial y = 9 \times 10^{-4}$ and 2.5×10^{-3} m s^{-1}, respectively, in order to maintain a relative humidity of around 90% at both catalyst layers.

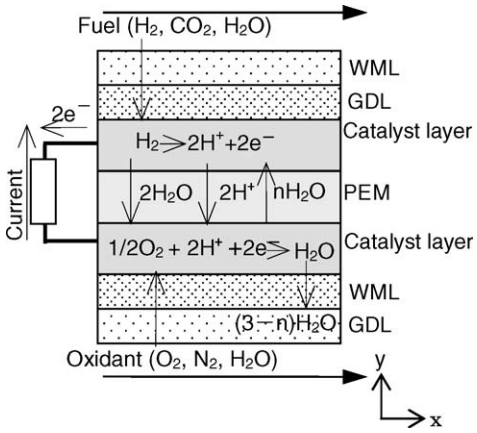

Fig. 2. Model of mass transfer in PEFC.

4. Simulation analysis for water vapor permeation test

A water vapor permeation test was conducted in order to search for materials and fabrication methods for the GDL and WML-deposited GDL. These layers are supposed to achieve a low humidification membrane electrode assembly (MEA), as obtained by the analysis in Section 3. The same simulator as that in Section 3 was used, and the simulation analysis was conducted by simulating the water vapor permeation rate test described in Section 5.

4.1. Analysis conditions

The analysis conditions are shown in Table 2. The vapor permeation area was 3 cm × 15 cm in accordance with the vapor permeation rate test, and the test pressure was atmospheric pressure. The temperature of the gas flow channel was 80 °C, and the vapor chamber was filled with air at 100% relative humidity at 70 °C.

4.2. Analysis results

Fig. 3 shows the relationship between the vapor permeation rate, which was obtained by the simulation analysis of the water vapor permeation test, and the vapor diffusion coefficient, $D/\partial y$, of Eq. (1). As shown in the figure, $D/\partial y = 9 \times 10^{-4}$ m s^{-1} at the oxidant inlet, which was obtained from Fig. 3, corresponds to the vapor permeation rate of 0.016 mol s^{-1} m^{-2}, and $D/\partial y = 2.5 \times 10^{-3}$ m s^{-1} at the oxidant outlet corresponds to the vapor permeation rate of 0.040 mol s^{-1} m^{-2}.

Table 2
Analysis conditions for water vapor permeation test

Vapor permeation area	0.03 m × 0.15 m
Experimental pressure	Ambient
Gas channel	
Temperature (°C)	80
Fluid	Dry air
Flow rate	0.5×10^{-3}, 1×10^{-3}, 1.5×10^{-3} m^3 min^{-1}
Vapor chamber	
Temperature (°C)	70
Fluid	Air (RH 100%)

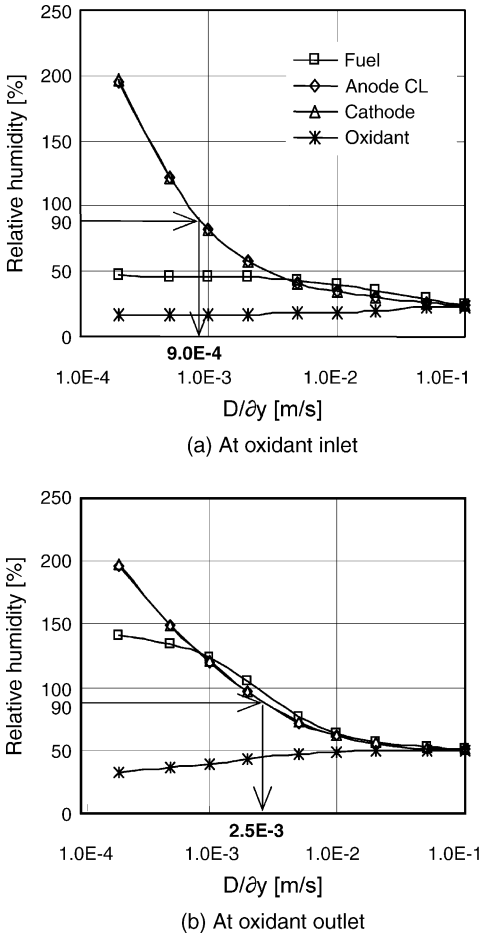

Fig. 3. Relationship between RH and $D/\partial y$ obtained by cell simulation analysis.

5. Test for vapor permeation rate through WML-coated GDL

The water vapor permeation test, which was conducted in the simulation in Section 4, was carried out with actual GDL or WML-coated GDL materials as parameters. Thus, the GDL and WML-coated GDL that can achieve a low humidification cell were experimentally determined.

5.1. Test method

The test apparatus used to evaluate the vapor permeation rate through the GDL and the WML-coated GDL is shown in Fig. 4 [19]. Pure water at 70 °C was held in a container in the test apparatus. The GDL or the WML-coated GDL was placed above the container and a gas flow channel was set above them. Next, dry air was passed though the gas flow channel and the amount of water vapor that passed through the GDL or the WML-coated GDL was measured using a condenser installed on the outlet side.

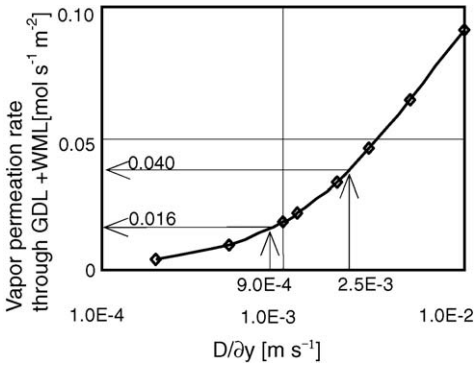

Fig. 4. Relationship between vapor permeation rate through GDL + WML and $D/\partial y$.

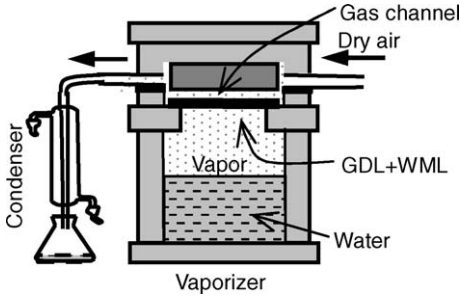

Fig. 5. Experimental apparatus for evaluating the vapor permeation rate through the GDL + WML.

5.2. Test results

The test results displayed in Fig. 5 depict the relationship between the vapor permeation rate and the air flow rate. The vapor permeation was significantly reduced by coating WML onto the GDL. Based on the results of Figs. 3 and 5, a prototype cell for the power generation test was prepared as follows. In order to satisfy the simulation results, WML(b)-coated GDL was installed at the oxidant inlet of the cathode to 1/3, WML(a)-coated GDL was installed from 1/3 to 2/3, and only GDL was installed from 2/3 to the oxidant outlet.

6. Power generation test

Sections 3 through 5 demonstrated that a low humidification cell is possible by coating a WML that has a gradient in the vapor permeation rate onto the GDL. In this section, a power generation test on a small single cell containing such a gradient WML is described.

6.1. Method for power generation test

The conceptual diagrams for two kinds of cells used in the test are shown in Fig. 6. Fig. 6(a) displays a cell in which WMLs are uniformly applied to both the anode side and the cathode side. Fig. 6(b) depicts a cell that reflects the results in Section 5, with the vapor permeation rate of the WML having a gradient along the direction of the oxidant flow.

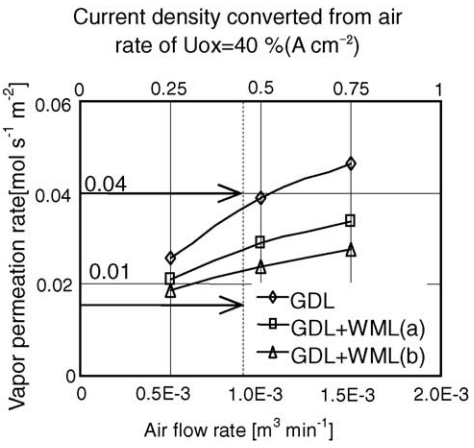

Fig. 6. Vapor permeation test result of GDL + WML.

The power generation conditions are shown in Table 3. During the power generation, the cell temperature was maintained at 80 °C under atmospheric pressure. A simulation gas of the methane reforming was supplied in 70% utilization as a fuel and air was supplied in 40% utilization as an oxidant. The fuel and oxidant feedstreams were humidified, in advance, to a dew point of 40, 50, 60, or 70 °C.

6.2. Results for power generation test

Figs. 7 and 8 show the power generation test results of the cell with a uniform WML and the cell with a gradient WML, respectively. Parts (a) and (b) of both the figures show the *I–V* characteristics and the cell internal resistances for various oxidant humidification temperatures (HT), respectively. It is thought that the internal resistance is one of the measures which show the water uptake amount of an electrolyte membrane. In parts (a) and (b) of both figure, the cell with a gradient WML can generate higher cell voltages and has higher water uptakes than that of a uniform WML at lower humidification. These results verify that the cell designed by the method of Section 3 can keep its catalyst layers in high humidity only by generation water. Adversely, as shown in Fig. 8(a), the cell of HT 70 °C shows an interiority performance to the cell of HT 60 °C in the region of high current density. This means that the exces-

Table 3
Condition of power generation test

Active area	0.03 m × 0.15 m
Operating pressure	Ambient
Cell temperature (°C)	80
Fuel	
Gas composition	$H_2 + CO_2$ (20%)
Utilization	70%
Humidification temperature (°C)	40, 50, 60, 70
Oxidant	
Gas composition	Air
Utilization (%)	40
Humidification temperature (°C)	40, 50, 60, 70

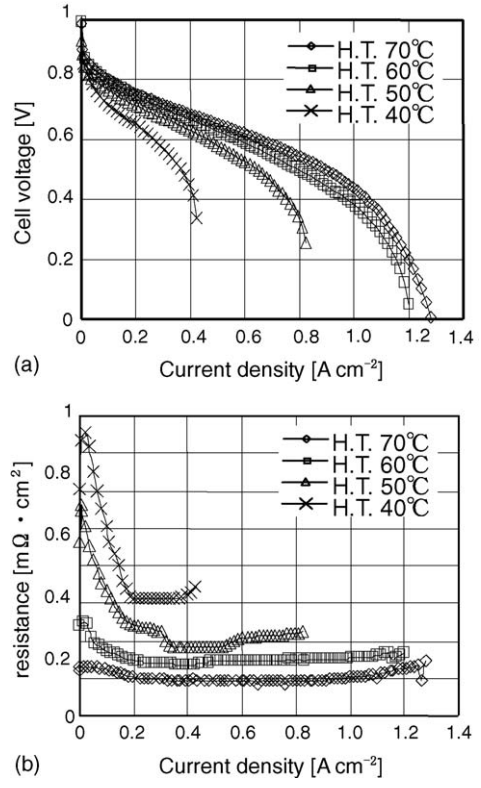

Fig. 7. Performance of the water-managed cell with uniform WML.

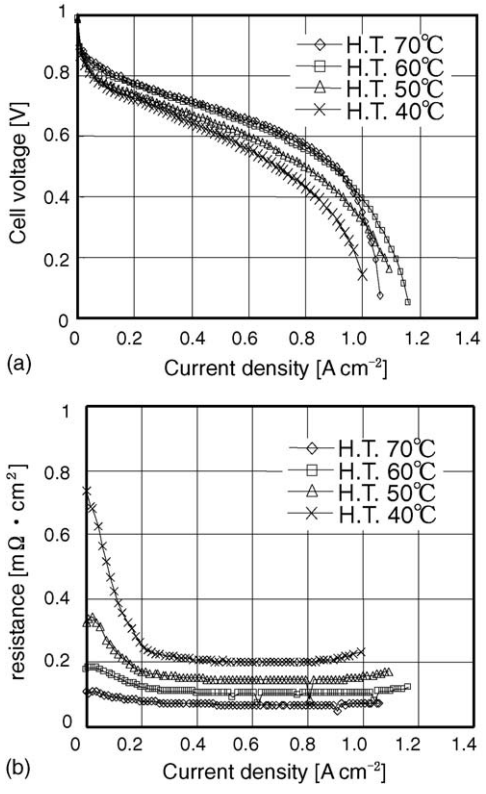

Fig. 8. Performance of the water-managed cell with gradient WML.

sive water retention of the cell with a gradient WML causes to flooding.

As is clear from a comparison of the figures, the cell performance at low humidification temperatures is significantly improved when the gradient WML is used. These results verify the validity of the design method for the water management, which was described in Sections 3 through 5, and shows that sufficient cell performance can be achieved a low humidity of 40 °C.

7. Conclusion

The cell simulator demonstrated that WML-coated GDL enabled the operation of a cell at low or no humidity. A small single cell containing the WML-coated GDL achieved a high level of performance under the quasi-non-humidification, which experimentally verified the validity of water management process using the cell simulator.

Acknowledgments

This study was supported by the research and development of polymer electrolyte fuel cell project of the New Energy and Industrial Technology Development Organization (NEDO), Japan and was conducted jointly with Toshiba Fuel Cell Power Systems Corporation.

References

[1] J.A. Kerres, J. Membr. Sci. 185 (2001) 3–27.
[2] S.D. Knights, K.M. Colbow, J. St-Pierre, D.P. Wilkinson, J. Power Sources 127 (2004) 127–134.
[3] J. Freire, E. Gonzalez, J. Electroanal. Chem. 503 (2001) 57–68.
[4] D. Picot, R. Metkemeijer, J.J. Bezian, L.R. Rouveyre, J. Power Sources 75 (1998) 251–260.
[5] D.L. Wood, J.S. Yip, T.V. Nguyen, Electrochim. Acta 43 (1998) 3795–3809.
[6] A. Yoshimura, H. Maeda, H. Fukumoto, K. Mitsuda, O. Hiroi, Fuel Cell Seminar (2002) 50–52.
[7] H. Maeda, A. Yoshimura, H. Fukumoto, K. Mitsuda, The Ninth FCDIC Fuel Cell Symposium Proceedings, 2002, pp. 87–90.
[8] L. Jordan, A. Shukla, T. Behrsing, N. Avery, B. Muddle, M. Forsyth, J. Power Sources 86 (2000) 250–254.
[9] M.W. Fowler, R. Mann, J. Amphiett, B. Peppley, P.R. Roberge, J. Power Sources 106 (2002) 274–283.
[10] R. Jiang, D. Chu, J. Power Sources 92 (2001) 193–198.
[11] D.P. Wilkinson, J. St-Pierre, J. Power Sources 114 (2003) 70–79.
[12] H.H. Voss, D.P. Wilkinson, P.G. Pickup, M.C. Johnson, V. Basura, Electrochim. Acta 40 (1995) 321–328.
[13] T. Nguyen, M. Knobbe, J. Power Sources 114 (2003) 70–79.
[14] Z. Qi, A. Kaufman, J. Power Sources 109 (2002) 38–46.
[15] V. Mehta, J. Cooper, J. Power Sources 114 (2003) 32–53.
[16] E. Antolini, R. Passos, E.A. Ticianelli, J. Appl. Electrochem. 32 (2002) 383–388.
[17] S. Shimotori, K. Saito, M. Hori, Proceedings of the 34th Intersociety Engineering Conference on Energy Conversion, 1999.
[18] T. Matsuura, M. Kato, M. Hori, Trans. Jpn. Soc. Mech. Eng. 71 (2005) 209–214.
[19] J. Chen, T. Matsuura, M. Hori, J. Power Sources 131 (2004) 155–161.
[20] Japan Society of Mechanical Engineers, JSME Mechanical Engineer's Hand book A6-145.